  Hydrology Research | 48.3 | 2017

From (cyber)space to ground: new technologies for smart farming

Giovanni Ravazzani, Chiara Corbari, Alessandro Ceppi, Mouna Feki, Marco Mancini, Fabrizio Ferrari, Roberta Gianfreda, Roberto Colombo, Mirko Ginocchi, Stefania Meucci, Daniele De Vecchi, Fabio Dell'Acqua and Giovanna Ober

ABSTRACT

Increased water demand and climate change impacts have recently enhanced the need to improve water resources management, even in those areas which traditionally have an abundant supply of water, such as the Po Valley in northern Italy. The highest consumption of water is devoted to irrigation for agricultural production, and so it is in this area that efforts have to be focused to study possible interventions. Meeting and optimizing the consumption of water for irrigation also means making more resources available for drinking water and industrial use, and maintaining an optimal state of the environment. In this study we show the effectiveness of the combined use of numerical weather predictions and hydrological modelling to forecast soil moisture and crop water requirement in order to optimize irrigation scheduling. This system combines state of the art mathematical models and new technologies for environmental monitoring, merging ground observed data with Earth observations from space and unconventional information from the cyberspace through crowdsourcing.

Key words | crowdsourcing, hydrological model, irrigation management, satellite observations, soil moisture, weather forecast

Giovanni Ravazzani (corresponding author)
Chiara Corbari
Alessandro Ceppi
Mouna Feki
Marco Mancini
Department of Civil and Environmental Engineering,
Politecnico di Milano,
Piazza Leonardo da Vinci 32,
Milano 20133, Italy
E-mail: *giovanni.ravazzani@polimi.it*

Fabrizio Ferrari
Roberta Gianfreda
Terraria srl, via Melchiorre Gioia 132,
Milano 20125, Italy

Roberto Colombo
Mirko Ginocchi
Remote Sensing of Environmental Dynamics Laboratory, DISAT,
University of Milano Bicocca,
Piazza della Scienza 1,
Milano 20126, Italy

Stefania Meucci
MMI srl, via Daniele Crespi 7,
Milano 20123, Italy

Daniele De Vecchi
Fabio Dell'Acqua
Department of Industrial and Information Engineering,
University of Pavia, via Ferrata 5,
Pavia 27100, Italy

Giovanna Ober
CGS S.p.A., Via Gallarate 150,
Milano 20151, Italy

INTRODUCTION

Despite growing slower than in the recent past, the world population is projected to increase by more than one billion people within the next 15 years, reaching 8.5 billion in 2030, and to increase a further 9.7 billion in 2050 and 11.2 billion by 2100 (United Nations Department of Economic and Social Affairs Population Division 2015). Growth in population and income will imply a substantial increase in demand for water and food – not only due to a higher number of people, but also to trends towards more water demanding lifestyles and diets. The agricultural sector is going to face enormous challenges in order to sustain food production, which is required to increase by 70% by 2050.

Additional factors, such as climate change, will further contribute to affect water availability. Changes of average

doi: 10.2166/nh.2016.112

precipitation will not be uniform, with some regions experiencing increases, and others decreases, or not much change at all (Ravazzani *et al.* 2014a). According to climate projections, the Mediterranean area should be affected by a decrease of total precipitation with the exception of the Alps in winter (Coppola & Giorgi 2010). With earlier snow melting and rainfall variation, inter-annual run-off is changing towards less water during summer but more water during winter (Dedieu *et al.* 2014; Gaudard *et al.* 2014). This would negatively alter the current seasonal cycle of runoff, even in those areas where mean annual precipitation is expected to remain steady with negative impacts on agricultural production.

The increase in consumption of water resources, combined with climate change impacts, calls for new sources of water supply (Ravazzani *et al.* 2011) and/or different managements of available resources in agriculture. One way to increase the quality and quantity of agricultural production is using modern technology to make farms more 'intelligent', the so-called 'precision agriculture' also known as 'smart farming'.

The scientific literature provides some studies focused on 'smart farming' by coupling meteorological and hydrological models (Gowing & Ejieji 2001; Cai *et al.* 2007). Ceppi *et al.* (2014) demonstrated that in-advance prediction of soil moisture (SM) and crop water requirement allows a precise irrigation scheduling with benefits on farmer income in terms of reduction of water consumption and increase of crop yield. However, their investigation was funded on local analysis in one single cultivated site where ground measurements of meteorological and hydrological variables were acquired hourly. Moreover, they used only temperature forecast to predict evaporation by applying an empirical model (Ravazzani *et al.* 2012). Open issues still remain about how to extend application to larger areas, and how physically based methods that are fed the complete set of meteorological variables can improve SM forecast.

Spatially distributed, physically based hydrological models, with their ability to estimate energy and water fluxes at the agricultural district scale, are invaluable tools for water resources management for agricultural water use (Corbari *et al.* 2015). Satellite data, for their intrinsic raster structure, can be effectively used for the internal calibration/validation of distributed hydrological models in each pixel of the domain. This can be achieved with those models based on energy and water balance algorithms in combination with remotely sensed data, in particular of land surface temperature (LST) (Corbari & Mancini 2014).

The information content of satellite images may be useful not only in providing a temporal dataset to calibrate and validate hydrological models, but even for assessment of biophysical attributes, such as leaf area index (LAI) (Colombo *et al.* 2003) and surface albedo (Corbari *et al.* 2014), and their temporal variation (Mattar *et al.* 2014). Thus, the combined use of physically raster-based hydrological models and satellite data may be an answer to the question about extending prediction to larger ungauged areas.

However, not all necessary information can be derived from satellite-based Earth observation. For example, vegetation height is an important piece of information, but it is rarely used due to challenges in its extraction. Therefore, crowdsourcing becomes a valid, integrative source of information, leveraging on the popularity of smartphones and tablets. Examples of applied crowdsourcing can be found in different topics, from fire mapping (Goodchild & Glennon 2010) to risk management purposes (Bevington *et al.* 2012).

Sophisticated physically based hydrological models need more meteorological variables to compute water and energy fluxes. Besides the fact that full meteorological observations are not always available with sufficient spatial density, questions arise about reliability of meteorological prediction by weather forecast models that are needed for SM and crop water requirement forecast (Ceppi *et al.* 2013). Many studies have been devoted to analyze the accuracy of precipitation forecast and performance of hydro-meteorological coupled systems, mainly for the purpose of flood forecasting (Amengual *et al.* 2008; Rabuffetti *et al.* 2008; Ceppi *et al.* 2010; Pianosi & Ravazzani 2010; Senatore *et al.* 2015; Arnault *et al.* 2016; Larsen *et al.* 2016). However, accuracy of the forecast of other meteorological variables except precipitation and performance of meteo-hydrological systems for SM forecast still need in-depth investigation.

The aim of this paper is to assess how mathematical models for weather and hydrological simulations, together with new technologies in the field of Earth observation from space and technologies for getting information from cyberspace (crowdsourcing), can help managing irrigation scheduling in a rich cultivated area in northern Italy. This work was part of the SEGUICI project, an Italian acronym that stands for smart technologies for water resources management for civil consumption and irrigation.

MATERIALS AND METHODS

Study area

The studied area is the Muzza Bassa Lodigiana (MBL) consortium in the middle of the Po Valley, close to the city of Lodi. The territory of the MBL covers an area of 740 km^2 where there are over 150 irrigation basins and thousands of irrigation sub-basins with individual fields of landowners (Figure 1).

The Muzza canal (about 40 km long) derives water from the Adda river at Cassano d'Adda and it flows back into the Adda river close to Castiglione d'Adda. Along the canal there are 38 intakes and many more hydraulic nodes; the entire Muzza network is composed by open earth canals. The Muzza is both the largest irrigation canal by capacity and the first artificial canal built in northern Italy.

Average annual rainfall in the MBL consortium ranges between 800 (southern area) and 1,000 mm (northern area) with two peaks in spring and autumn (Ceriani & Carelli 2000). Winter is generally cold with a mean monthly temperature of 2 °C in January and summer is hot and humid with a mean monthly temperature of 23.4 °C in July (ERSAF 2004). Evapotranspiration (ET) amounts can reach up to 500 mm during the summer season, therefore, most of the water supply for agriculture comes from the irrigation network.

In the period 2010–2012 one test-site of the Pre.G.I. project (Prediction and Guiding Irrigation) (Ceppi *et al.* 2014) was located in the central area of the basin at Cascina Nuova farm, in Livraga town. Here, one meteorological and one eddy-covariance station and time-domain reflectometry (TDR) probes were installed to measure mass and energy exchanges between soil, plant and atmosphere (Masseroni *et al.* 2012, 2013; Corbari *et al.* 2013).

In 2015, the monitoring station was moved from Livraga to Secugnago site (Figure 1). In both the monitored fields, farmers cultivated corn and flood irrigation was scheduled by the MBL consortium according to planned water allotments that were determined in advance. Landowners cannot irrigate their fields on days other than the scheduled ones (the Italian name of this irrigation scheduling method is *turno irriguo*). On average, farmers can irrigate fields once every 2 weeks.

Specific field campaigns were performed in order to characterize soil properties. Soil water retention curve parameters for Livraga and Secugnago are reported in Table 1. Sampling points were selected randomly within

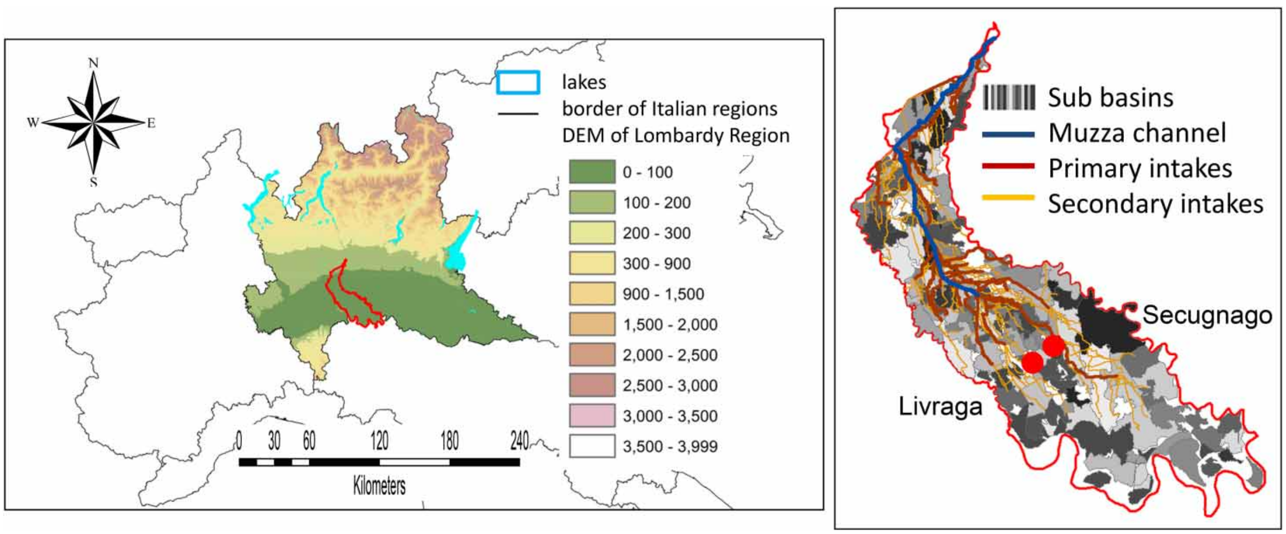

Figure 1 | The Lombardy region in the north of Italy (left) and the Muzza basin with its irrigation sub-basins (right).

both study sites. Samples were collected from different depths. The parameters presented in Table 1 are average values. Particle size distribution for each soil sample was determined by wet sieving and hydrometer method. Sand, silt and clay contents together with soil texture were identified according to the United States Department of Agriculture system of soil classification. Undisturbed soil samples were used to measure the saturated hydraulic conductivity following the falling-head method (Lee et al. 1985). Soil water retention curve parameters were defined through evaporation method experiments (Wendroth et al. 1993) using the Hydraulic Property Analyzer device. Results were afterwards fitted to the Brooks & Corey (1964) parametric equation.

Satellite observations

In order to obtain a spatial estimation of some biophysical parameters (normalized difference vegetation index, NDVI; LAI; fractional cover, FC; albedo) and of the hydrological model variable LST over the Muzza basin, remote sensing data acquired from the moderate resolution imaging spectroradiometer (MODIS) were chosen, and in particular, two types of surface reflectance data (from Collection-5 MODIS/Terra Land Products) used, namely, MO09GQ and MOD09GA, both already atmospherically corrected for vegetation parameters' retrieval. Data from the MODIS near real-time (NRT) context were used.

As regards MOD09GQ, surface reflectance data in Bands 1 (red spectral range) and 2 (near infrared spectral range) were used, daily provided at a 250-m spatial resolution. As regards MOD09GA, surface reflectance data from Bands 1 to 7 (from visible to infrared spectral range), daily provided at a 500-m spatial resolution, and a specific dataset of reflectance data state quality assurance (to generate cloud-cover masks), daily provided at a 1,000-m spatial resolution, were used.

Table 1 | Soil water retention curve parameters for Livraga and Secugnago sites

Parameter	Livraga	Secugnago
Saturated water content [m^3/m^3]	0.389	0.379
Residual water content [m^3/m^3]	0.015	0.051
Field capacity [m^3/m^3]	0.33	0.301
Wilting point [m^3/m^3]	0.133	0.179
Saturated conductivity [m/s]	2.36×10^{-7}	6.79×10^{-6}
Brooks and Corey pore size index [–]	0.234	0.509
% Sand	32.73	71.94
% Silt	48.08	22.43
% Clay	19.19	5.63
Soil texture	Loam	Sandy loam

First, by means of a binary mask (0-1) identifying the study area and a land-cover map of Lombardy region, a time-invariant mask referred to Muzza basin was created, wherein a numerical value from 1 to 3 was assigned to every pixel, thus carrying information about the corresponding land-use class (i.e., crops, grasslands and agro-foresty areas; pixel not falling under these three classes were set to NaN).

MOD09GQ and MOD09GA products were initially converted from their original sinusoidal projection to UTM Zone 32N WGS-84, with a pixel size of 250 m, by using MODIS Reprojection Tool in batch mode.

In order to improve parameter estimation quality, a time-variant cloud-cover mask was daily created from the reflectance data state quality assurance dataset. Then, spatial maps of NDVI, FC, LAI and albedo were created for that day-of-year (DOY) throughout the study area.

Reflectance (ρ) data in Bands 1 (R) and 2 (NIR) of MOD09GQ product were used for NDVI calculation over the study area, according to the classic formula:

$$NDVI = \frac{\rho_{NIR} - \rho_R}{\rho_{NIR} + \rho_R} \tag{1}$$

The resulting matrix was weighed with the cloud-cover mask (resampled at 250-m pixel size) generated for that DOY; each pixel of NDVI matrix maintained its value only if the corresponding pixel of cloud-cover mask was 1 (i.e., cloud-clear and cloud-shadow free), otherwise NDVI value was set to NaN. All the following analyses were carried out only if the percentage of cloud-pixels was lower than 50%, otherwise no map was created for the given DOY. Moreover, for every class, minimum and maximum NDVI values ($ndvi_{MIN}$ and $ndvi_{MAX}$) were computed by selecting (through frequency histogram calculation, assuming a uni-modal distribution) the lowest and the highest NDVI values, respectively, with a frequency of more than a certain threshold (e.g., 0.5% for crops class, which is the largest one).

Then, maps of FC were calculated for every class, according to the empirical formula proposed by Richter &

Timmermans (2009):

$$FC = 1 - \left(\frac{ndvi_{MAX} - ndvi}{ndvi_{MAX} - ndvi_{MIN}}\right)^{p} \quad (2)$$

with p set to 0.9 (Campbell & Norman 1998); $ndvi_{MAX}$ and $ndvi_{MIN}$ (calculated as described above) are assumed to be NDVI values of a surface fully covered and completely uncovered by vegetation, respectively.

By using FC values thus obtained, maps of LAI were calculated for every class, according to Choudhury (1987):

$$LAI = -\frac{\ln(1 - fc)}{0.5} \quad (3)$$

For the albedo, reflectance data of bands from 1 to 7 were used (Liang 2000):

$$\begin{aligned} ALBEDO = {} & 0.039\rho_{B1} + 0.504\rho_{B2} - 0.071\rho_{B3} \\ & + 0.105\rho_{B4} + 0.252\rho_{B5} + 0.069\rho_{B6} \\ & + 0.101\rho_{B7} \end{aligned} \quad (4)$$

Finally, we generated the 8-day composites of FC, LAI and albedo: every day and for each of the three parameters, the map effectively returned as output is composed of pixels whose values are the maximum values that appeared over the last 8 days.

The LST variable was also derived from NRT satellite imagery, for which MOD11_L2 product was used with a 1,000-m spatial resolution.

Meteorological forecast

The Weather Research and Forecasting-Advance Research WRF version 3.61 (WRF-ARW) meteorological model was used to generate daily meteorological forecasts with a forecast horizon of 9 days and a temporal resolution of 1 hour. These weather outputs were used to drive the 1-day hydrological simulations. Meteorological fields from the National Center for Environmental Prediction (NCEP) Global Forecasting System with $0.25^{\circ} \times 0.25^{\circ}$ resolution were used as initial and boundary conditions. For this study, the WRF computation domains comprise the whole of Italy with 18×18 km horizontal resolution (58×68 horizontal grid cells) and 28 vertical layers. A second domain has been created with higher resolution, 3×3 km (25×25 grid cells) nested within the national domain (Figure 2). The quite small size of the second domain was selected in order to keep the computational time within acceptable limits, and still provide satisfactory modelling results.

The model was set up using single-moment 6-class microphysics scheme (WSM6) containing ice, snow and graupel processes (Hong & Lim 2006), the Noah land surface model scheme (Tewari *et al.* 2004), the PBL Yonsei University (YSU) scheme (Hong *et al.* 2006) and the CAM scheme for radiation (Collins *et al.* 2004).

To improve the estimation of the initial values, observations were assimilated in the model using WRFDA system (Barker *et al.* 2012) with 3DVAR techniques (Barker *et al.* 2004). Data taken in were derived from NCEP database and include: satellite radiances in BUFR format and conventional observations from land, ocean and upper-air platforms in PREPBUFR format.

Other weather data (temperature, wind speed, wind direction and pressure) were taken from meteorological stations of the Meteonetwork database.

Finally, albedo and LAI data derived from satellite observations of land cover were used to replace standard values in WRF simulations for the higher resolution domain.

Hydrological modelling

Two distributed hydrological models were used for simulating the water balance components: the flash-flood event-based spatially distributed rainfall–runoff transformation, including water balance (FEST-WB) (Rabuffetti *et al.* (2008)) and the flash-flood event-based spatially distributed rainfall–runoff transformation, including energy and water balance (FEST-EWB) (Corbari *et al.* (2011)). The primary difference between them is in the computation of ET. The FEST-WB model derives the actual ET by rescaling the potential ET using a simple empirical approximation, where the potential ET is computed based only on air temperature measurements (Ravazzani *et al.* 2012, 2014a). In contrast, the FEST-EWB model computes the actual ET by solving the system of water mass and energy balance equations (Ravazzani *et al.* 2014a). The differences in the input parameters and meteorological forcings are listed in Table 2.

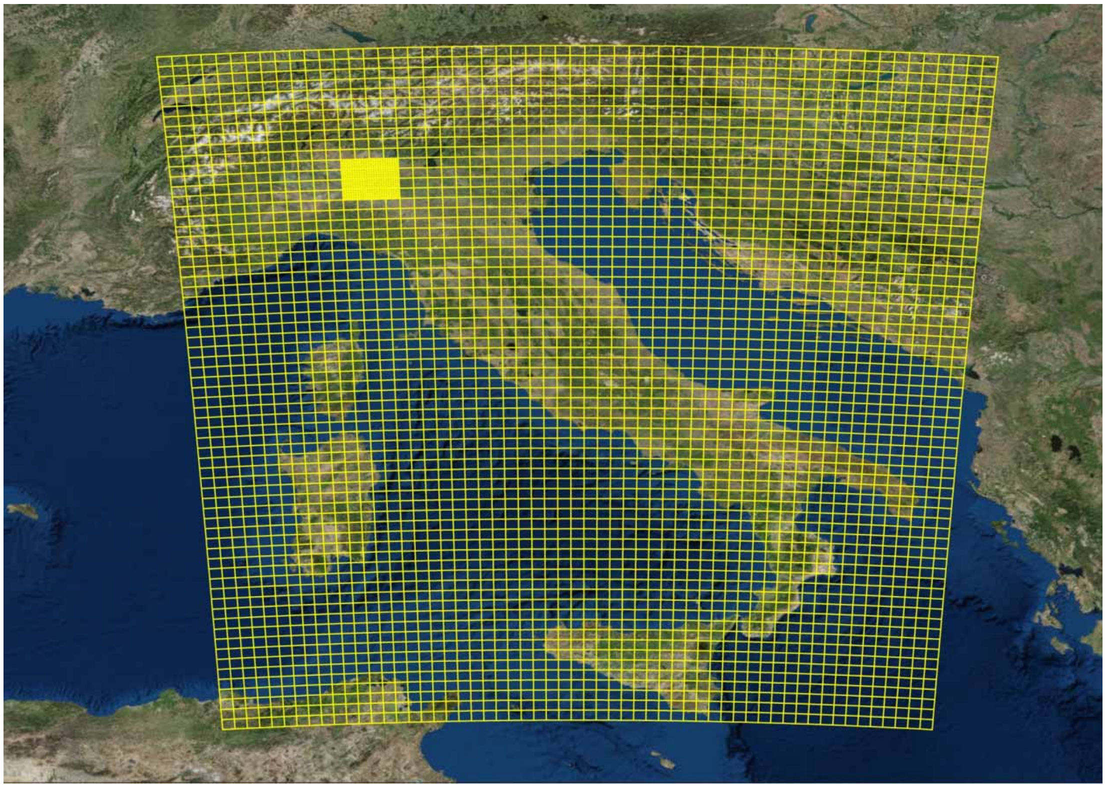

Figure 2 | WRF simulation domains.

Both models discretize the computation domain with a mesh of regular square cells (200×200 m in this study), in each of which water fluxes are calculated at hourly time step.

In particular, SM dynamics, θ, for the generic cell at position i, j, is described by the water balance equation:

$$\frac{\partial \theta_{i,j}}{\partial t} = \frac{1}{Z_{i,j}}(P_{i,j} - R_{i,j} - D_{i,j} - ET_{i,j}) \tag{5}$$

where P is the precipitation rate, R is runoff flux, D is drainage flux, ET is evapotranspiration rate and Z is the soil depth. For further details on distributed hydrological models and their applications, readers may refer to Boscarello *et al.* (2014) and Ravazzani *et al.* (2014b, 2014c, 2015).

Crowdsourcing

Based on the idea of volunteers ('citizen sensors') providing information through their smartphones, a mobile app was designed to collect vegetation-related parameters (Figure 3(a)).

The idea is to let everyone collect useful information, even contributors without a specific background; therefore, pictures of the most commonly found vegetation species are included as examples, to guide the end-users in deciding what species they have just taken a picture of. The mobile app allows including the height of vegetation, directly related to the stage of growth, and if the field is flooded or not, useful information to know whether the farmer is irrigating the field.

Every collected report, which includes a geocoded and oriented picture and answers to the above-mentioned group of questions, is automatically uploaded and stored in a remote database (Galeazzo *et al.* 2015). To avoid weighing on the contributor's mobile data quota, an option can be activated to store reports on the hand-held device and upload them only when a WiFi connection becomes available. A webgis interface is used to display data on an OpenStreetMap-based map (Figure 3(b)). Within the

Table 2 | Meteorological forcings and parameters used as input to the FEST-WB and FEST-EWB models

Input	Unit	FEST-WB	FEST-EWB
Precipitation	mm	X	X
Temperature	°C	X	X
Solar radiation	W/m^2		X
Wind speed	m/s		X
Relative humidity	%		X
Saturated hydraulic conductivity	m/s	X	X
Residual moisture content	–	X	X
Saturated moisture content	–	X	X
Wilting point	–	X	X
Field capacity	–	X	X
Pore size index	–	X	X
Curve number	–	X	X
Soil depth	M	X	X
Vegetation fraction	%	X	X
Crop coefficient	–	X	
LAI	m^2/m^2		X
Albedo	–		X
Minimum stomatal resistance	s/m		X
Vegetation height	M		X

server, an algorithm can automatically associate the geo-localized reports with polygons related to each single field using Global Positioning System (GPS) position and compass direction (Figure 3(c)). Cooperation is in progress with the Research Support Service of the European Space Agency to share the collected data for their possible use in validation of land cover/use information derived from Earth observation satellite datasets.

RESULTS AND DISCUSSION

Performance of the hydrological models

The FEST-EWB and the FEST-WB models were calibrated and validated following different procedures. In fact, the FEST-EWB model was calibrated distributed by comparison of simulated LST with the observed ones and validated against local SM and ET, whereas the FEST-WB model was calibrated locally and SM and ET were measured.

Calibration and validation of the FEST-WB model

The 2010–2011 period was used to calibrate and the 2012 to validate the FEST-WB model against SM and ET observations acquired at Cascina Nuova field in Livraga. Only values of the parameters of the cell corresponding to the station site could be calibrated as there were no other stations with similar capabilities available in the consortium. Figure 7 shows the comparison between observed and simulated SM and ET, along with rainfall and irrigation amount, during the three growing seasons of 2010, 2011 and 2012.

In general, satisfactory results are found in terms both of SM and ET during calibration and validation periods. More details and comments can be found in Ceppi *et al.* (2014).

Calibration and validation of the FEST-EWB model

The FEST-EWB model was calibrated during the period 2010–2012 against observed MODIS LST. Hence, soil hydraulic and vegetation parameters were calibrated in each single pixel minimizing the difference between the observed and simulated land surface temperatures, following the procedure developed by Corbari & Mancini (2014) and Corbari *et al.* (2015). For the entire dataset of 166 images, statistical parameters between LST from calibrated FEST-EWB and LST from MODIS were computed: mean absolute error (MAE) is equal to 0.2 °C, root mean square error to 1.8 °C, relative error (RE) to 4.2% and the Nash & Sutcliffe (1970) index to 0.73. Cities areas were discarded from the comparison. In Figure 5, as an example, for 27 August 2012 at 13:00, MODIS LST and FEST-EWB LST images before and after the calibration, are shown.

The FEST-EWB model was then validated against the fluxes measured acquired at Cascina Nuova field in Livraga. In Figure 4, cumulated ET over the 3 years was reported for observed data and for the calibrated FEST-EWB. A RE of 5.6% was found between observations and ET from the calibrated model, while a RE of 44.1% was obtained if the non-calibrated ET was considered. SM estimates had a mean RE of 5.9%.

In general, the hydrological model FEST-EWB, after the calibration procedure, is able to correctly reproduce distributed LST and local SM and ET during calibration and

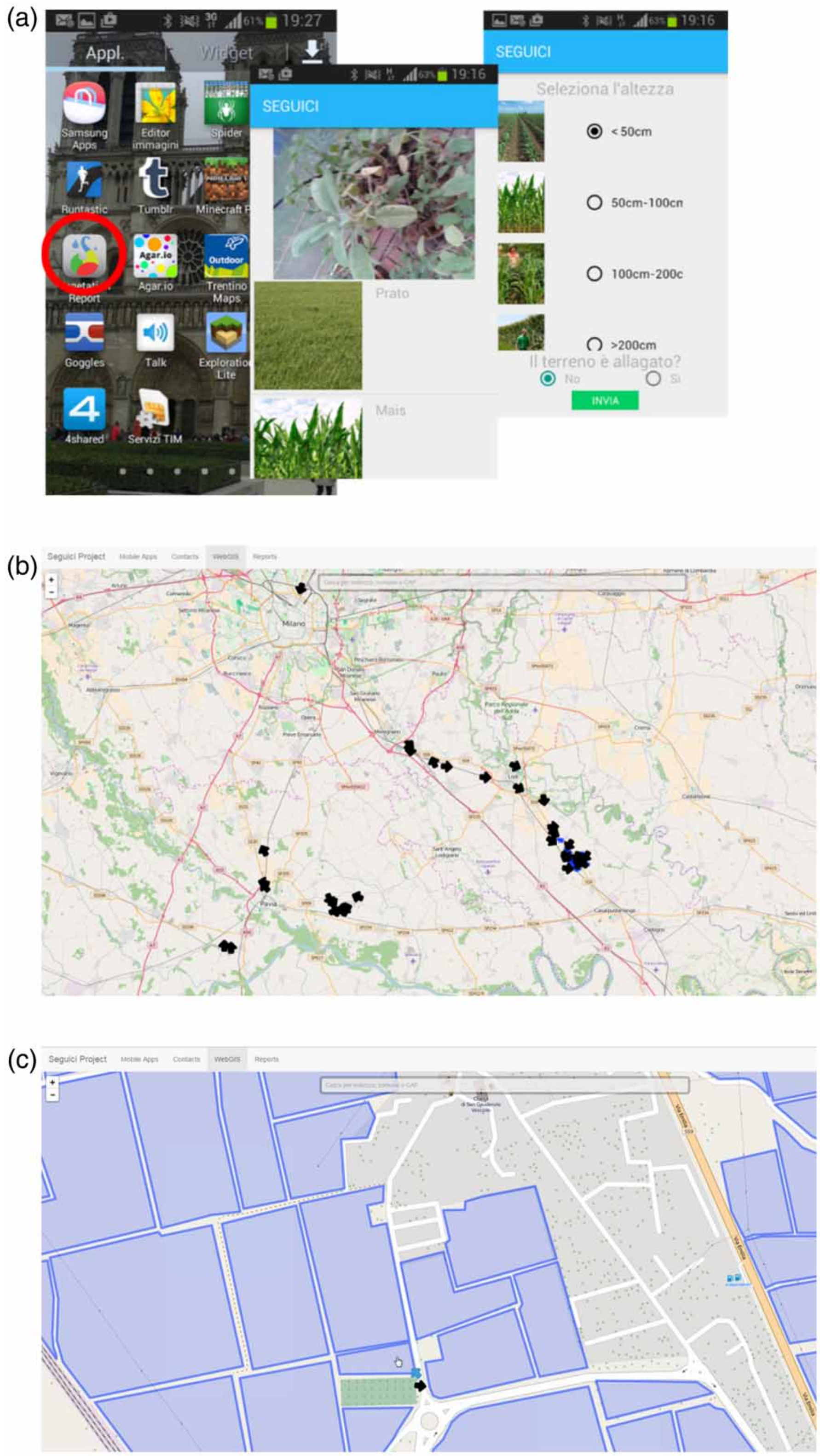

Figure 3 | Mobile app graphic interface (a), WebGIS interface (b), and detail of automatic association of a report with the corresponding polygon according to compass direction (c).

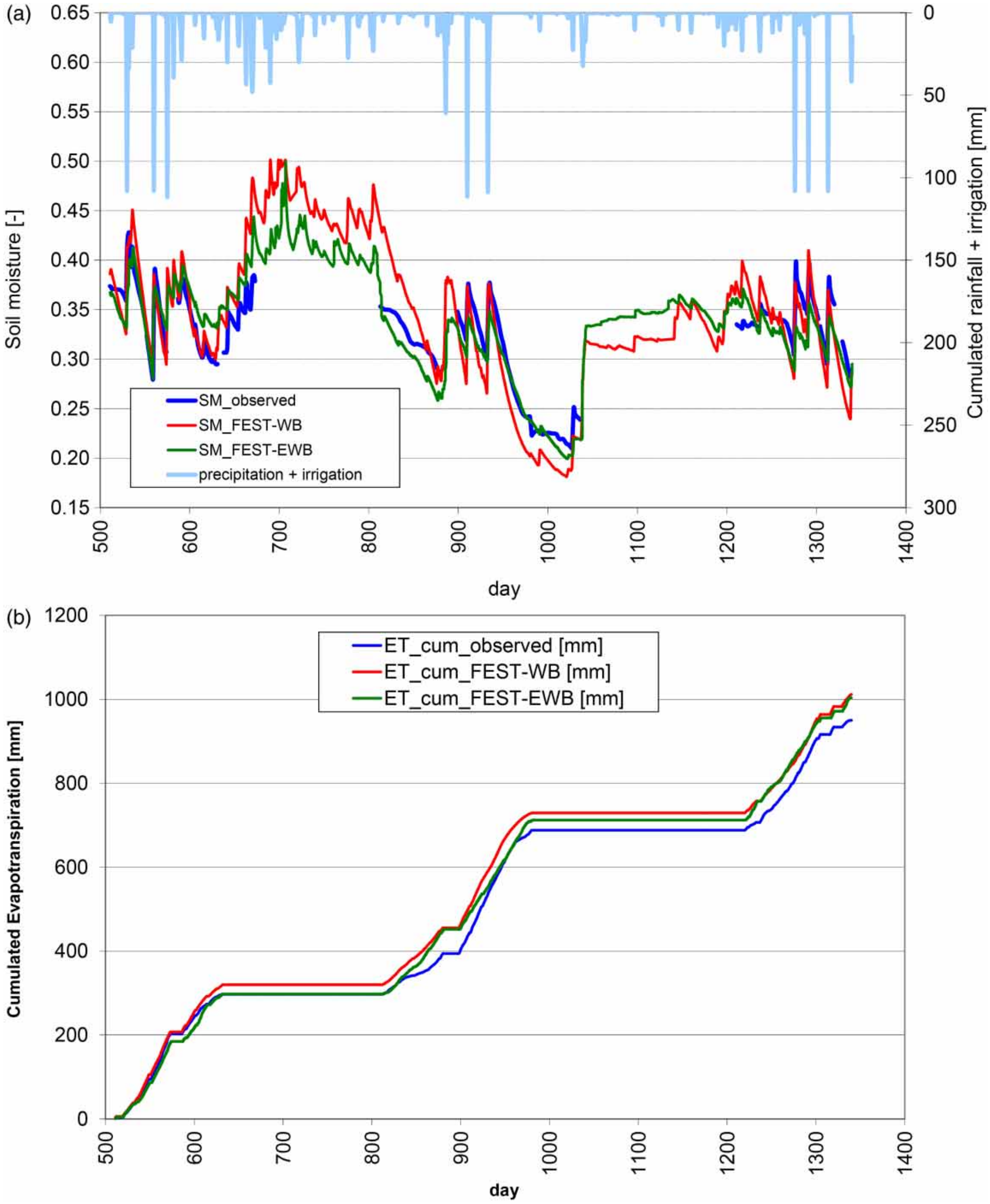

Figure 4 | Comparison between observed and simulated SM and ET at Livraga during 2010–2012.

validation periods (Figure 5). More details of this case study can be found in Corbari *et al.* (2013).

Comparison between the FEST-WB and the FEST-EWB models

SM and ET estimates from FEST-EWB and FEST-WB were then compared at local and basin scales for 2015. The simulations of both models for the 2015 growing season were performed without a local calibration, but using their own parameters previously calibrated for 2010. Hence, FEST-WB soil parameters were only locally (e.g., Livraga) calibrated, while FEST-EWB ones were calibrated in a distributed way for each pixel of the analysed domain.

Figure 6 shows the comparison between observed and simulated SM and ET, along with rainfall and irrigation, at

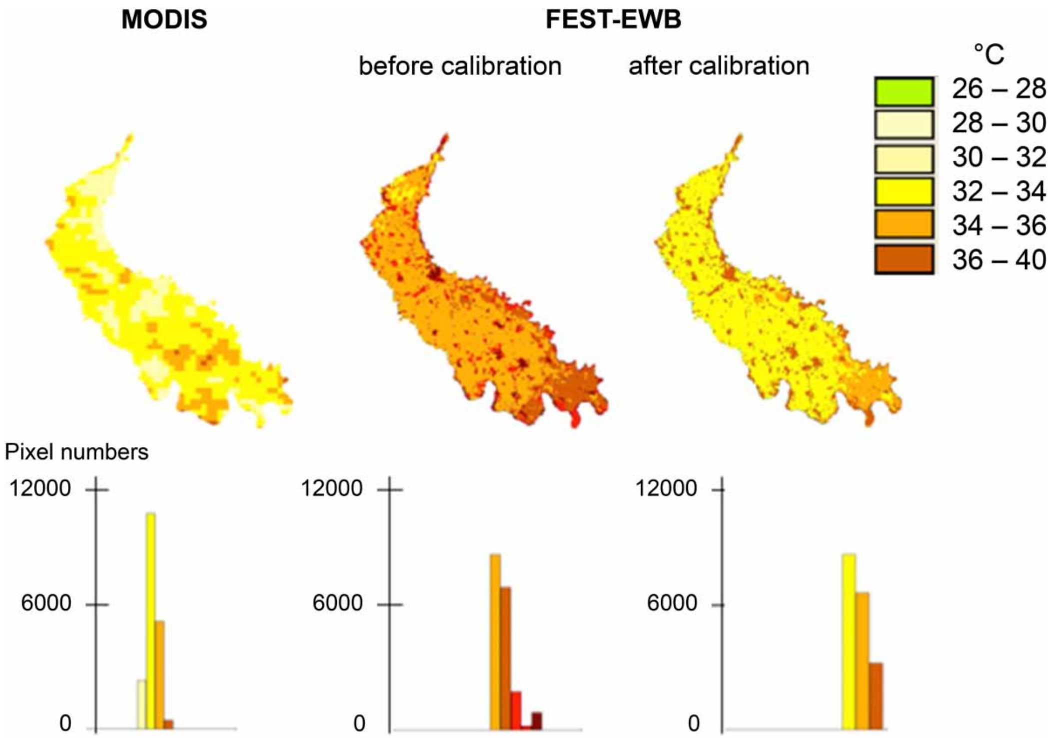

Figure 5 | MODIS LST and RET images reported for the O-SoVeg configuration and after calibration for 27 August 2012 at 13:00.

Secugnago station. SM from FEST-EWB better reproduces observed SM with a mean RE equal to 0.6% and a Nash & Sutcliffe (1970) index equal to 0.78. In contrast, SM from FEST-WB has a mean RE of 18.5% with observed data and a Nash & Sutcliffe (1970) index equal to −0.13. Hence, SM from FEST-EWB and FEST-WB has a relative difference of 21.4%.

Observed ET at Secugnago site was available concurrently to model simulations only from Day 154 (3 June) to Day 171 (21 June) due to station malfunctioning. Cumulated ET from FEST-EWB and from FEST-WB were then compared with observed values until 21 June and a RE equal to 0.69% and to −7% was obtained, respectively (Figure 6). The difference between the two models in computing ET over the whole growing season was equal to 42.7 mm.

FEST-EWB results were also compared at basin scale in each pixel of the domain with the output of the simplified version of FEST-WB in terms of SM and ET. In Figure 7, for 30 September 2015, maps and histograms of simulated SM and ET from FEST-EWB and FEST-WB are reported. The SM spatial mean for FEST-EWB is equal to 0.22 with a standard deviation of 0.09, and for FEST-WB are 0.17 and 0.077, respectively. If all the maps are analysed from 3 June to 30 September 2015, the mean temporal differences of the spatial mean is equal to 0.08.

The same comparison was then performed for ET maps. In Figure 7, as an example, the FEST-EWB and FEST-WB maps are reported for 30 September 2015 at 12:00. ET spatial mean and standard deviation are equal to 0.13 mm and 0.05 mm for FEST-EWB, while for FEST-WB they are equal to 0.037 mm and 0.01 mm.

When the entire simulation period is considered, the mean temporal differences of the spatial mean is equal to 1.1 mm. These differences are due to different modelling schemes on ET and calibration procedures; in particular, the FEST-WB was calibrated at local scale only, while the FEST-EWB was calibrated pixel by pixel at basin scale.

Impact of crowdsourcing data

In order to assess how crowdsourcing data may affect accuracy of water balance, SM and ET were simulated with

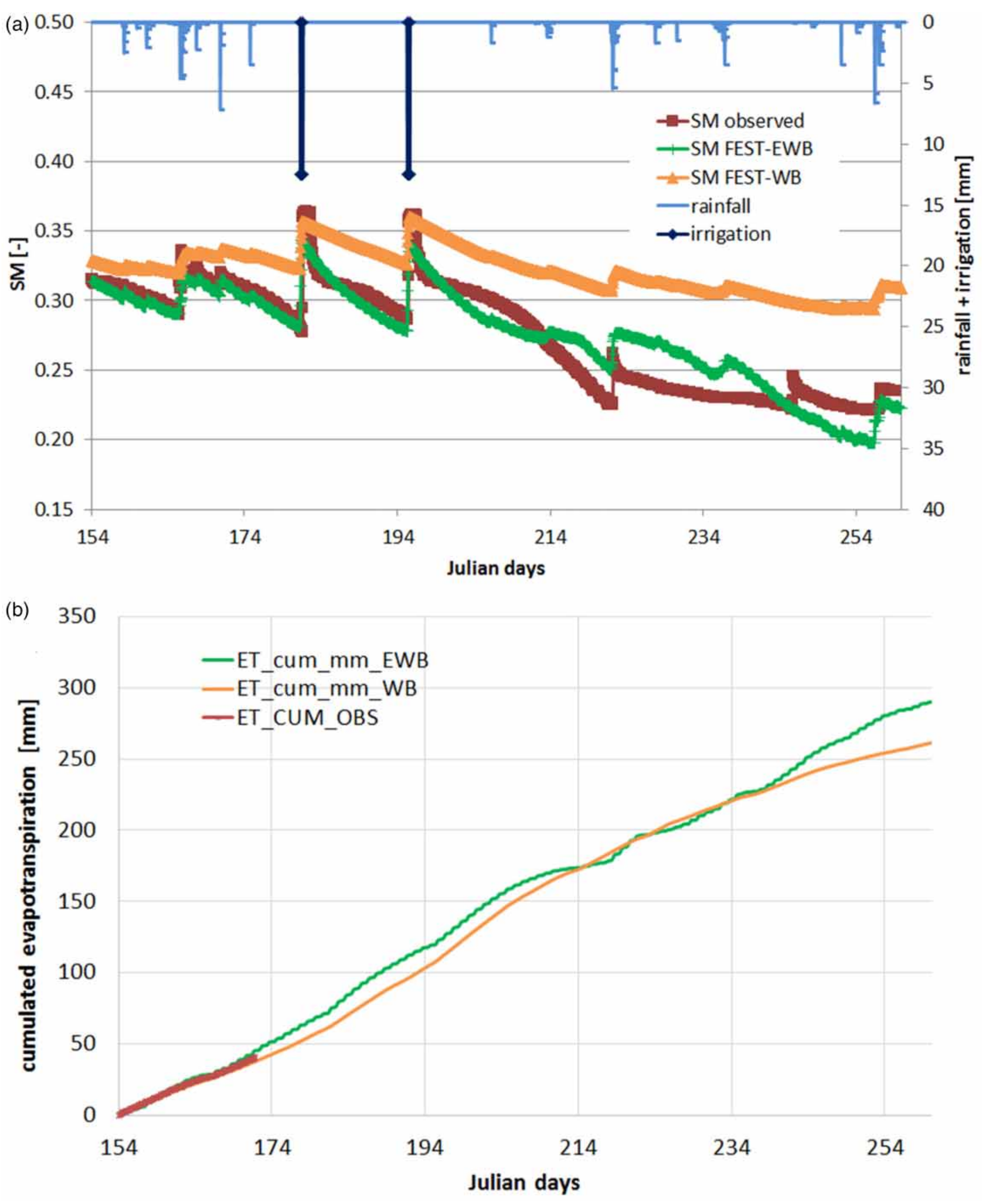

Figure 6 | Comparison between observed and simulated SM and ET at Secugnago during 2015.

FEST-EWB at the Secugnago site according to three scenarios:

1. Vegetation weight was changed according to crowd-sourcing information acquired with the smartphone application, LAI and albedo were retrieved from remotely sensed images, and crop minimum stomatal resistance (rsmin) was set to 150 s/m. This is the reference scenario whose results were presented in previous sections.
2. We assume the field was grass cultivated, and all vegetation parameters were assigned for a grass crop: height = 0.12 m, LAI = 1, rsmin = 70 s/m.
3. We assume the field was grass cultivated, height = 0.12, rsmin = 70 s/m, but LAI and albedo were taken from remotely sensed images.

Results are shown in Figure 8. Scenario 2 exhibits a significant difference with respect to the reference

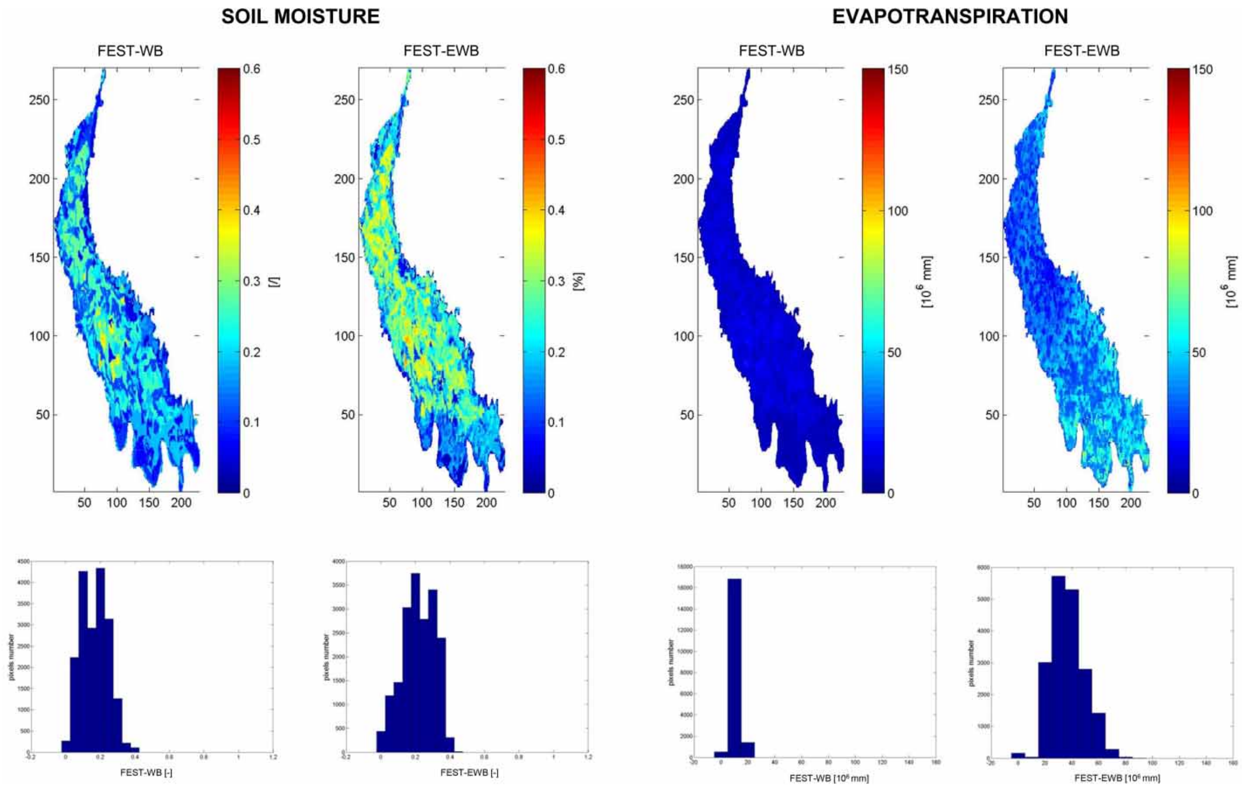

Figure 7 | Comparison of maps and histograms between simulated SM and ET from FEST-EWB and FEST-WB for 30 September 2015.

scenario, which means that water balance simulation may lose accuracy if the type of plant that is cultivated and its phenology are not known. The difference between scenario 3 and the reference scenario is lower because information retrieved from remotely sensed images can substantially compensate the lack of information about cultivated plants. As a general comment, the difference is greater when water supply is not enough to sustain ET and this is limited by vegetation parameters.

Verification of the weather predictions

The WRF meteorological model was daily launched from 3 June 2015 to 30 September 2015 in order to obtain weather forecasts over the two areas of study during the 2015 growing season. The main meteorological fields available to feed the FEST hydrological models were: air temperature and relative humidity, incoming shortwave solar radiation, precipitation and wind speed.

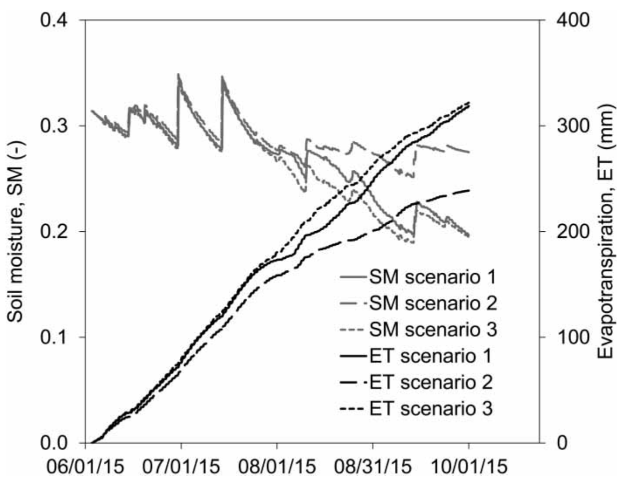

Figure 8 | Comparison of SM and cumulated ET simulated under three different scenarios as described in the section 'Comparison between the FEST-WB and the FEST-EWB models'.

Table 3 highlights the performance of the WRF model forecasts in comparison with observed data for the entire forecast horizon of 9 days over the Secugnago site. The forecast of the *day +0*, i.e., the forecast of the same day of the model initialization, is here omitted, since it would not be exploitable for irrigation scheduling management.

Satisfactory results were found over the Secugnago test-bed during the 4 months of simulations. In fact, air temperature forecasts maintained a bias of about 2 °C for the entire forecast horizon; in particular, the WRF model tended to underestimate temperatures and even relative humidity forecasts were 6–8% below the observed data; in contrast, the incoming solar radiation, wind speed and daily precipitation were overestimated by the WRF model at about 80–90 W/m^2, 1.6–1.8 m/s and 2–7 mm, respectively. In general, no outliers were found during the analysed period and no significant decrement of the WRF performance at increasing of lead-time was present.

SM forecast and irrigation scheduling

Weather forecasts were afterwards used to drive the FEST hydrological model simulations using the two schemes (ET computed with Hargreaves equation, FEST-WB; and ET computed by solving the energy balance, FEST-EWB) for calculating SM at Livraga and Secugnago sites. Goodness of forecast was assessed by computing literature fit indexes comparing SM simulated by FEST-WB and FEST-EWB fed with observed meteorological forcings and SM obtained with the same hydrological models fed with meteorological forecasts.

As shown in Tables 4 and 5, a better correlation (R^2) was found using the energy-balance model in both the two sites, Livraga and Secugnago, respectively; however, the MAE for SM shows fairly good results using both the Hargreaves and energy-balance equations during the entire forecast horizon, also due to a good performance of weather forecasts previously described; acceptable values, in fact, were found between 0.01 and 0.03 from *day +0* to *day +8*, respectively.

The benefit of having a good coupled hydro-meteorological system many days in advance can be summarized in

Table 3 | MAE for the WRF meteorological model over the Secugnago area from *day +1* to *day +8* as lead time of forecast

MAE	*Day +1*	*Day +2*	*Day +3*	*Day +4*	*Day +5*	*Day +6*	*Day +7*	*Day +8*
Temperature [°C]	2.43	2.25	2.2	2.17	2.12	2.00	1.94	2.27
Relative humidity [–]	0.06	0.06	0.06	0.06	0.07	0.07	0.08	0.08
Daily precipitation [mm]	2.23	1.87	3.02	3.15	2.77	3.70	6.70	5.48
Incoming solar radiation [W/m^2]	81.04	80.79	80.57	83.58	84.18	90.34	84.75	87.49
Wind speed [m/s]	1.65	1.63	1.71	1.61	1.60	1.58	1.67	1.77

Table 4 | Performance for SM forecasts over the Livraga maize field using Hargreaves equation (a) and the energy balance (b)

Livraga	*d + 0*	*d + 1*	*d + 2*	*d + 3*	*d + 4*	*d + 5*	*d + 6*	*d + 7*	*d + 8*
(a)									
SM – Hargreaves									
R^2 [–]	0.88	0.80	0.81	0.80	0.75	0.70	0.68	0.63	0.54
MAE	0.01	0.01	0.01	0.01	0.02	0.02	0.02	0.02	0.03
MRE [%]	2.89%	3.99%	4.11%	4.61%	5.49%	5.81%	6.30%	7.59%	9.23%
(b)									
SM – EWB									
R^2 [–]	0.94	0.88	0.88	0.86	0.82	0.78	0.75	0.71	0.63
MAE	0.00	0.00	0.00	0.00	0.00	0.00	0.01	0.01	0.01
MRE [%]	0.32%	0.38%	0.19%	0.08%	0.04%	−0.10%	−0.22%	−0.21%	−0.11%

Table 5 | Performance for SM forecast over the Secugnago maize field using Hargreaves equation (a) and the energy balance (b)

Secugnago	d + 0	d + 1	d + 2	d + 3	d + 4	d + 5	d + 6	d + 7	d + 8
(a)									
SM – Hargreaves									
R^2 [–]	0.80	0.70	0.71	0.68	0.62	0.56	0.51	0.45	0.36
MAE	0.00	0.01	0.01	0.01	0.01	0.01	0.01	0.01	0.01
MRE [%]	0.83%	1.18%	1.27%	1.49%	1.67%	1.75%	2.04%	2.41%	2.90%
(b)									
SM – EWB									
R^2 [–]	0.92	0.85	0.86	0.84	0.78	0.74	0.69	0.62	0.50
MAE	0.01	0.01	0.01	0.01	0.02	0.02	0.02	0.03	0.03
MRE [%]	0.69%	0.18%	−0.88%	−1.65%	−2.28%	−3.17%	−3.62%	−3.79%	−3.58%

the following picture where a reanalysis for the period 22 June 2015 to 15 July 2015 is shown. In this time span, according to the MBL consortium regulation, irrigation was scheduled on 30 June 2015 and 14 July 2015.

Figure 9 shows accumulated precipitation and SM forecasts initialized 1 day before (dashed lines) and 8 days before (solid lines) the planned irrigation of 30 June. The FEST-EWB simulation, under the assumption that no irrigation occurred, is included as well. This demonstrates that irrigation scheduled on 30 June was necessary in order to maintain SM above stress threshold, since no significant rainfall was predicted before the next planned irrigation allotment of 14 July, with a consequent high risk of compromising the crop.

SUMMARY AND CONCLUSIONS

This work was part of the SEGUICI project, the aim of which was to develop and integrate smart technologies for water resources management for civil consumption and irrigation.

The aim of this paper was to assess how mathematical models for weather and hydrological simulations, together with remotely sensed images and crowdsourcing, can help in managing irrigation scheduling, by forecasting SM and crop water requirement. The test beds of the project were two maize fields at Livraga (2010–2012) and Secugnago (2015) in the MBL consortium, about 50 km south-east of Milan in northern Italy.

The SM forecast was accomplished by coupling a meteorological model with the FEST hydrological model. Numerical weather predictions were provided by the WRF-ARW meteorological model with a 10-day lead-time. Two configurations of the FEST distributed hydrological model were tested: the FEST-WB scheme that computes ET with the Hargreaves equation, and the FEST-EWB that solves the energy balance equation.

The FEST-WB model was calibrated against SM and actual ET measured at Livraga station during the 2010–2012 campaigns. Only parameters of the cells surrounding the Livraga station could be calibrated as no other measurements were available in the MBL area. The FEST-EWB model was calibrated during the period 2010–2012 against observed MODIS LST. The two models were further validated against SM measured in the 2015 campaign at Secugnago. Comparisons with observations show that, while FEST-EWB was able to properly simulate SM and ET, FEST-WB, which was not calibrated at Secugnago, showed greater error. Moreover, the comparison of spatial distribution of SM and ET computed by FEST-WB and FEST-EWB showed significant differences due to different methods used for their calibration. Calibration using remotely sensed images is an effective alternative to ground-based observations and provides spatially distributed information impossible to acquire with conventional technologies.

Crowdsourcing resulted in a fundamental source of information that could increase the accuracy of water balance simulation, with maximum advantage occurring when combined with remotely sensed information.

The performances of numerical weather predictions were assessed against air temperature and relative

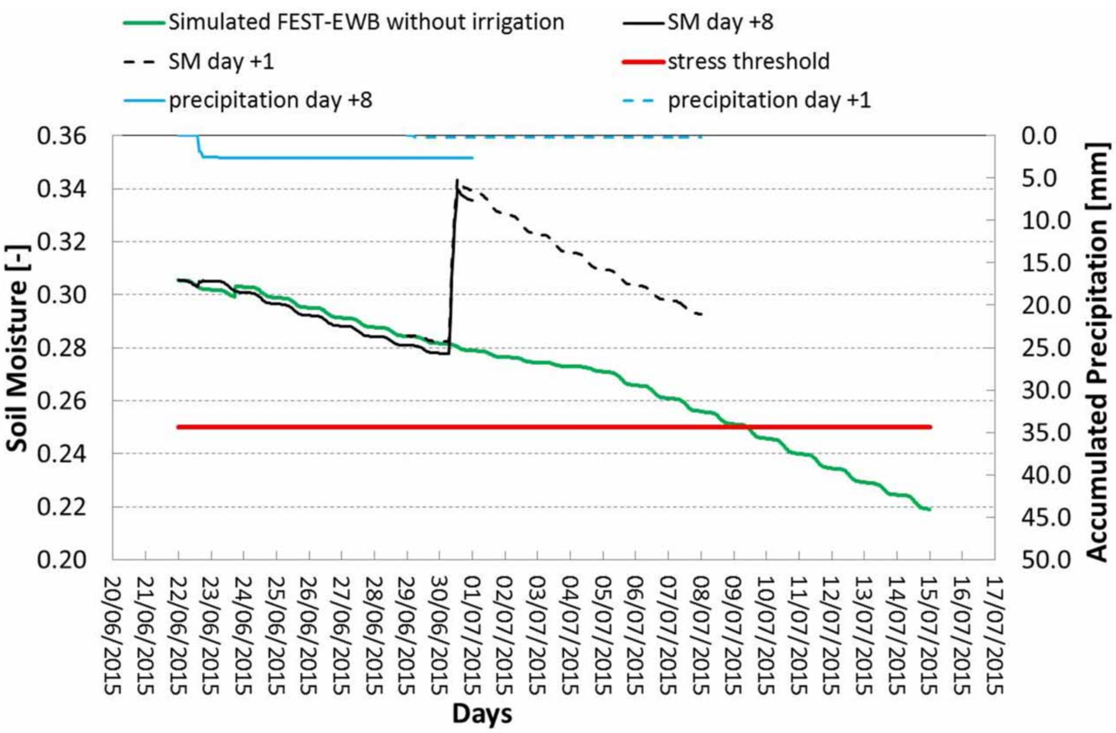

Figure 9 | Simulation of the FEST-EWB model without the scheduled irrigation of 30 June; accumulated precipitation and SM forecast by the WRF model initialized 8 days (solid lines) and 1 day (dashed lines) before the planned irrigation.

humidity, incoming shortwave solar radiation, precipitation and wind speed observations at Secugnago. Air temperature forecasts maintained a bias of about 2 °C for the entire forecast horizon; in particular, the WRF model tended to underestimate temperatures and even relative humidity forecasts were 6–8% below the observed data. In contrast, the incoming solar radiation, wind speed and daily precipitation were overestimated by the WRF model at about 80–90 W/m^2, 1.6–1.8 m/s and 2–7 mm, respectively.

Weather forecasts were afterwards used to drive the FEST-WB and FEST-EWB models for forecasting SM at Livraga and Secugnago in the 2015 campaign. Goodness of forecast was assessed by computing literature fit indexes comparing SM simulated by FEST-WB and FEST-EWB fed with observed meteorological forcings and SM obtained with the same hydrological models fed with meteorological forecasts. SM forecast was reasonably satisfactory no matter whether the FEST-WB or the FEST-EWB was used. Moreover, results showed how combing meteorological and hydrological model that were correctly calibrated, it was possible to get reliable SM forecasts for up to 1 week, and this helped farmers to properly decide irrigation scheduling.

ACKNOWLEDGEMENTS

This work was sponsored by the Lombardy region in the framework of the SEGUICI project. We thank ARPA Lombardia (http://www.arpalombardia.it) and the Meteonetwork Association (http://www.meteonetwork.it) for providing meteorological observations from automatic stations. The editor, Prof. Attilio Castellarin, and three anonymous reviewers are gratefully acknowledged for their efforts to improve the quality and contents of this manuscript.

REFERENCES

Amengual, A., Diomede, T., Marsigli, C., Martín, A., Morgillo, A., Romero, R., Papetti, P. & Alonso, S. 2008 A hydrometeorological model intercomparison as a tool to quantify the forecast uncertainty in a medium size basin. *Natural Hazards and Earth System Sciences* **8**, 819–838.

Arnault, J., Wagner, S., Rummler, T., Fersch, B., Bliefernicht, J., Andresen, S. & Kunstmann, H. 2016 Role of runoff-infiltration partitioning and resolved overland flow on land-atmosphere feedbacks: a case study with the WRF-Hydro Coupled Modeling System for West Africa. *Journal of Hydrometeorology*. DOI: http://dx.doi.org/10.1175/JHM-D-15-0089.1.

Barker, D., Huang, X.-Y., Liu, Z., Auligné, T., Zhang, X., Rugg, S., Ajjaji, R., Bourgeois, A., Bray, J., Chen, Y., Demirtas, M., Guo, Y.-R., Henderson, T., Huang, W., Lin, H.-C., Michalakes, J., Rizvi, S. & Zhang, X. 2012 The weather research and forecasting model's community variational/ensemble data assimilation system: WRFDA. *Bulletin of the American Meteorological Society* **93**, 831–843.

Barker, D. M., Huang, W., Guo, Y.-R., Bourgeois, A. J. & Xiao, Q. N. 2004 A three-dimensional (3DVAR) data assimilation system for use with MM5: implementation and initial results. *Monthly Weather Review* **132**, 897–914.

Bevington, J., Eguchi, R., Huyck, C., Crowley, H., Dell'Acqua, F., Iannelli, G., Jordan, C., Morley, J., Wieland, M., Parolai, S., Pittore, M., Porter, K., Saito, K., Sarabandi, P., Wright, A. & Wyss, M. 2012 Exposure data development for the global earthquake model: inventory data capture tools. In: *15th World Conference on Earthquake Engineering, Lisbon, Portugal*.

Boscarello, L., Ravazzani, G., Rabuffetti, D. & Mancini, M. 2014 Integrating glaciers raster-based modelling in large catchments hydrological balance: the Rhone case study. *Hydrological Processes* **28** (3), 496–508. doi: 10.1002/hyp.9588.

Brooks, R. H. & Corey, A. T. 1964 *Hydraulic Properties of Porous Media*. Hydrolology Paper 3. Colorado State University, Fort Collins, CO, USA.

Cai, J., Liu, Y., Lei, T. & Pereira, L. S. 2007 Estimating reference evapotranspiration with the FAO Penman–Monteith equation using daily weather forecast messages. *Agricultural and Forest Meteorology* **145**, 22–35.

Campbell, G. S. & Norman, J. M. 1998 *An Introduction to Environmental Biophysics*. Springer, New York, 286 pp.

Ceppi, A., Ravazzani, G., Rabuffetti, D. & Mancini, M. 2010 Evaluating the uncertainty of hydrological model simulations coupled with metorological forecasts at different spatial scales. *Procedia – Social and Behavioral Sciences* **2** (6), 7631–7632.

Ceppi, A., Ravazzani, G., Salandin, A., Rabuffetti, D., Montani, A., Borgonovo, E. & Mancini, M. 2013 Effects of temperature on flood forecasting: analysis of an operative case study in Alpine basins. *Natural Hazards and Earth System Sciences* **13** (4), 1051–1062. doi: 10.5194/nhess-13-1051-2013.

Ceppi, A., Ravazzani, G., Corbari, C., Salerno, R., Meucci, S. & Mancini, M. 2014 Real time drought forecasting system for irrigation management. *Hydrology and Earth System Sciences* **18**, 3353–3366.

Ceriani, M. & Carelli, M. 2000 Maps of mean, maximum, and minimum annual precipitation over alpine area of Lombardy region, recorded in the period 1891–1990. *Geological Service, Office for Regional Geological Risk* (in Italian).

Choudhury, B. J. 1987 Relationships between vegetation indices, radiation absorption, and net photosynthesis evaluated by a sensitivity analysis. *Remote Sensing of Environment* **22**, 209–233.

Collins, W. D., Rasch, P. J., Boville, B. A., Hack, J. J., McCaa, J. R., Williamson, D. L., Kiehl, J. T., Briegleb, B., Bitz, C., Lin, S.-J., Zhang, M. & Dai, Y. 2004 *Description of the NCAR Community Atmosphere Model (CAM 3.0)*. NCAR Technical Note NCAR/TN–464 + STR. p. 214.

Colombo, R., Bellingeri, D., Fasolini, D. & Marino, C. M. 2003 Retrieval of leaf area index in different vegetation types using high resolution satellite data. *Remote Sensing of Environment* **86**, 120–131.

Coppola, E. & Giorgi, F. 2010 An assessment of temperature and precipitation change projections over Italy from recent global and regional climate model simulations. *International Journal of Climatology* **30**, 11–32.

Corbari, C. & Mancini, M. 2014 Calibration and validation of a distributed energy water balance model using satellite data of land surface temperature and ground discharge measurements. *Journal of Hydrometeorology* **15**, 376–392.

Corbari, C., Ravazzani, G. & Mancini, M. 2011 A distributed thermodynamic model for energy and mass balance computation: FEST-EWB. *Hydrological Processes* **25** (9), 1443–1452.

Corbari, C., Ravazzani, G., Ceppi, A. & Mancini, M. 2013 Multi-pixel calibration of a distributed energy water balance model using satellite data of land surface temperature and eddy covariance data. *Procedia Environmental Sciences* **19**, 285–292.

Corbari, C., Mancini, M., Su, Z. & Li, J. 2014 Evapotranspiration estimate from water balance closure using satellite data for the Upper Yangtze river basin. *Hydrology Research* **45**, 603–614.

Corbari, C., Mancini, M., Li, J. & Su, Z. 2015 Can satellite land surface temperature data be used similarly to ground discharge measurements for distributed hydrological model calibration? *Hydrological Sciences Journal* **60** (2), 202–217. doi: 10.1080/02626667.2013.866709.

Dedieu, J. P., Lessard-Fontaine, A., Ravazzani, G., Cremonese, E., Shalpykova, G. & Beniston, M. 2014 Shifting mountain snow patterns in a changing climate from remote sensing retrieval. *Science of the Total Environment* **493**, 1267–1279. doi: 10.1016/j.scitotenv.2014.04.078.

ERSAF (Regional Agency for Agriculture and Forest Services) 2004 *Soils and landscapes of the province of Lodi, Milan, February 2004* (in Italian). Available from: http://www.ersaf.lombardia.it/upload/ersaf/pubblicazioni/Suoli%20e%20paesaggi%20della%20provincia%20di%20Lodi_13383_408.pdf.

Galeazzo, D. A., De Vecchi, D., Dell'Acqua, F. & Demattei, P. 2015 A small step towards the citizen sensor: a multi-purpose framework for mobile apps. In: *Geoscience and Remote Sensing Symposium (IGARSS), 2015 IEEE International, Milan, Italy*, pp. 1348–1350. doi: 10.1109/IGARSS.2015.7326025.

Gaudard, L., Romerio, F., Dalla Valle, F., Gorret, R., Maran, S., Ravazzani, G., Stoffel, M. & Volonterio, M. 2014 Climate change impacts on hydropower in the Swiss and Italian Alps. *Science of the Total Environment* **493**, 1211–1221. doi: 10.1016/j.scitotenv.2013.10.012.

Goodchild, M. F. & Glennon, J. A. 2010 Crowdsourcing geographic information for disaster response: a research frontier. *International Journal of Digital Earth* **3** (3), 231–241. doi:10.1080/17538941003759255.

Gowing, J. W. & Ejieji, C. J. 2001 Real-time scheduling of supplemental irrigation for potatoes using a decision model and short term weather forecasts. *Agricultural Water Management* **47**, 137–153.

Hong, S.-Y. & Lim, J.-O. 2006 The WRF single-moment 6-class microphysics scheme (WSM6). *Journal of the Korean Meteorological Society* **42**, 129–151.

Hong, S.-Y., Noh, Y. & Dudhia, J. 2006 A new vertical diffusion package with an explicit treatment of entrainment processes. *Monthly Weather Review* **134**, 2318–2341.

Larsen, M. A. D., Christensen, J. H., Drews, M., Butts, M. B. & Refsgaard, J. C. 2016 Local control on precipitation in a fully coupled climate-hydrology model. *Scientific Reports* **6**, 22927. doi: 10.1038/srep22927.

Lee, D. M., Reynolds, W. D., Elrick, D. E. & Clothier, B. E. 1985 A comparison of three field methods for measuring saturated hydraulic conductivity. *Canadian Journal of Soil Science* **65** (3), 563–573.

Liang, S. 2000 Narrowband to broadband conversions of land surface albedo I algorithms. *Remote Sensing of Environment* **76**, 213–238.

Masseroni, D., Ravazzani, G., Corbari, C. & Mancini, M. 2012 Turbulence integral length and footprint dimension with reference to experimental data measured over maize cultivation in Po Valley, Italy. *Atmosfera* **25**, 183–198.

Masseroni, D., Corbari, C., Ceppi, A., Gandolfi, C. & Mancini, M. 2013 Operative use of eddy covariance measurements: are high frequency data indispensable? *Procedia Environmental Sciences* **19**, 293–302.

Mattar, C., Franch, B., Sobrino, J. A., Corbari, C., Jiménez-Muñoz, J. C., Olivera-Guerra, L., Skokovic, V., Sória, G., Oltra-Carriò, R., Julien, Y. & Mancini, M. 2014 Impacts of the broad-band albedo on actual evapotranspiration estimated by S-SEBI model over an agricultural area. *Remote Sensing of the Environment* **147**, 23–42.

Nash, J. E. & Sutcliffe, J. V. 1970 River flow forecasting through the conceptual models, Part 1: a discussion of principles. *Journal of Hydrology* **10** (3), 282–290.

Pianosi, F. & Ravazzani, G. 2010 Assessing rainfall-runoff models for the management of Lake Verbano. *Hydrological Processes* **24** (22), 3195–3205. doi:10.1002/hyp.7745.

Rabuffetti, D., Ravazzani, G., Corbari, C. & Mancini, M. 2008 Verification of operational Quantitative Discharge Forecast (QDF) for a regional warning system – the AMPHORE case studies in the upper Po River. *Natural Hazards and Earth System Sciences* **8**, 161–173.

Ravazzani, G., Giudici, I., Schmidt, C. & Mancini, M. 2011 Evaluating the potential of quarry lakes for supplemental irrigation. *Journal of Irrigation and Drainage Engineering* **137** (8), 564–571.

Ravazzani, G., Corbari, C., Morella, S., Gianoli, P. & Mancini, M. 2012 Modified Hargreaves-Samani equation for the assessment of reference evapotranspiration in Alpine river basins. *Journal of Irrigation and Drainage Engineering* **138**, 592–599.

Ravazzani, G., Ghilardi, M., Mendlik, T., Gobiet, A., Corbari, C. & Mancini, M. 2014a Investigation of climate change impact on water resources for an Alpine basin in Northern Italy: implications for evapotranspiration modeling complexity. *PLoS One* **9** (10), e109053. doi:10.1371/journal.pone.0109053.

Ravazzani, G., Gianoli, P., Meucci, S. & Mancini, M. 2014b Indirect estimation of design flood in urbanized river basins using a distributed hydrological model. *Journal of Hydrologic Engineering* **19** (1), 235–242. doi: 10.1061/(ASCE)HE.1943-5584.0000764.

Ravazzani, G., Gianoli, P., Meucci, S. & Mancini, M. 2014c Assessing downstream impacts of detention basins in urbanized river basins using a distributed hydrological model. *Water Resources Management* **28** (4), 1033–1044. doi: 10.1007/s11269-014-0532-3.

Ravazzani, G., Bocchiola, D., Groppelli, B., Soncini, A., Rulli, M. C., Colombo, F., Mancini, M. & Rosso, R. 2015 Continuous stream flow simulation for index flood estimation in an Alpine basin of Northern Italy. *Hydrological Sciences Journal* **60** (6), 1013–1025. doi: 10.1080/02626667.2014.916405.

Richter, K. & Timmermans, W. J. 2009 Physically based retrieval of crop characteristics for improved water use estimates. *Hydrology and Earth Systems Sciences* **13**, 663–674. doi:10.5194/hess-13-663-2009.

Senatore, A., Mendicino, G., Gochis, D. J., Yu, W., Yates, D. N. & Kunstmann, H. 2015 Fully coupled atmosphere-hydrology simulations for the central Mediterranean: impact of enhanced hydrological parameterization for short and long time scales. *Journal of Advances in Modelling Earth Systems* **7**, 1693–1715. doi:10.1002/2015MS000510.

Tewari, M., Chen, F., Wang, W., Dudhia, J., LeMone, M. A., Mitchell, K., Ek, M., Gayno, G., Wegiel, J. & Cuenca, R. H. 2004 Implementation and verification of the unified NOAH land surface model in the WRF model. In: *20th Conference on Weather Analysis and Forecasting/16th Conference on Numerical Weather Prediction*, pp. 11–15.

United Nations, Department of Economic and Social Affairs, Population Division 2015 *World Population Prospects: The 2015 Revision, Key Findings and Advance Tables*. ESA/P/WP.241.

Wendroth, O., Ehlers, W., Hopmans, J. W., Kage, H., Halbertsma, J. & Wosten, J. H. M. 1993 Reevaluation of the evaporation method for determining hydraulic functions in unsaturated soils. *Soil Science Society of America Journal* **57**, 1436–1443.

First received 15 April 2016; accepted in revised form 19 September 2016. Available online 5 December 2016